https://doi.org/10.37434/tpwj2022.04.05

FORMATION OF A JOINT BETWEEN DEPOSITED AND BASE METALS DURING LASER CLADDING OF A NICKEL-BASED POWDER ONTO A COPPER-BASED ALLOY

F. Bourahima[1,2], T. Baudin[2], M. Rege[1], V. Ji[2], F. Brisset[2], A. Zavdoveev[3], A.L. Helbert[2]

[1]Etablissements Chpolansky, 3 Rue Angiboust, 91 462 Marcoussis, France
[2]ICMMO, SP2M, Université Paris-Saclay, UMR CNRS 8182, bât.410, 91405 ORSAY, France
[3]E.O. Paton Electric Welding Institute of the NASU
11 Kazymyr Malevych Str., 03150, Kyiv, Ukraine

ABSTRACT

Laser cladding is an alternative method to other cladding techniques such as Plasma Transfer Arc (PTA) or blowtorch for surface treatment in the glass industry. It aims to produce dense, high-quality coatings on a non-planar surface without affecting its thermal and mechanical properties. In this study, Ni-based coatings were coated onto Cu–Ni–Al substrate using a 3 JET nozzle technique. During laser cladding, good metallurgical bonding is necessary to ensure the further surfacing process technique. A microstructural analysis was conducted, and the mechanical properties were then evaluated with microhardness analysis to link process parameters to coating bonding quality. A calculation of the power attenuation attempts to explain the impact of the powder distribution on the bonding. This work revealed that a chemical dilution zone exists between coating and substrate and is necessary for perfect metallurgical bonding. The heterogeneous bonding, observed through the section, along the curved interface coating/substrate, has been linked to the Gaussian distribution of the powder that attenuates the input power. The attenuated power was measured all along the interface.

KEYWORDS: laser cladding, power attenuation, powder distribution, dilution zone

INTRODUCTION

During glass bottle production, viscous glass is poured into Cupro–Nickel–Aluminum (Cu–Ni–Al) molds at temperatures ranging from 700 to 1200 °C. Cu–Ni–Al or cast-iron glass molds must absorb the high glass temperature to cool it homogeneously, playing the role of thermal exchangers [1]. However, during this process, corrosion or abrasion can appear on the molds' sensitive parts (neck ring and match). Also, thermal fatigue can be observed during the molding cycle. Therefore, it is important to modify the mold surface properties before the production to extend its lifespan. In order to do that, Ni-based or Co-based powder is cladded on those parts. The most famous cladding methods for glass industry are Plasma Transferred Arc (PTA) [2] and blowtorch [1]. But with these techniques, a high Heat Affected Zone (HAZ) is present. It corresponds to a zone belonging to the substrate that has not reached its fusion temperature but underwent a change in its structure due to the process. To avoid that, a pre-heating is operated with those techniques. In mold industry, the aim is to limit this Affected Zone to prevent changes in the substrate thermal properties. To be able to do that, laser cladding is operated instead of former techniques without mold pre-heating.

Laser cladding is an innovative surfacing technique, developed in the 90's [3,4]. It is used to obtain well-bonded high-quality materials, free of pores and cracks without affecting the substrate thermal properties (so, a low HAZ).

Some researchers have investigated the impact of laser cladding on the substrate microstructural change. In most of the studies, the HAZ is observed during laser cladding on cast iron substrates with the appearance of metastable phases like martensite or ledeburite [5, 6].

Balu et al. [7] have operated laser cladding with two kinds of Ni-based powder on Cu substrate with and without pre-heating. They observed that the grain size in the HAZ is high distanced from the interface. It has also been seen that this size increases at low laser scanning speed. Hardness is lower in the HAZ than distanced from the interface. They found that a substrate pre-heating leads to a better bonding due to a larger melting pool and HAZ.

Despite the limited HAZ, laser cladding often induces an area of local chemical dilution between the powder and the substrate. Authors explained that dilution is obtained at the interface when a fusion between the substrate and the coating occur [7–9]. This dilution, dependent on the input laser power [10], has to be restricted in order to avoid a large HAZ but seems necessary to ensure good metallurgical bond-

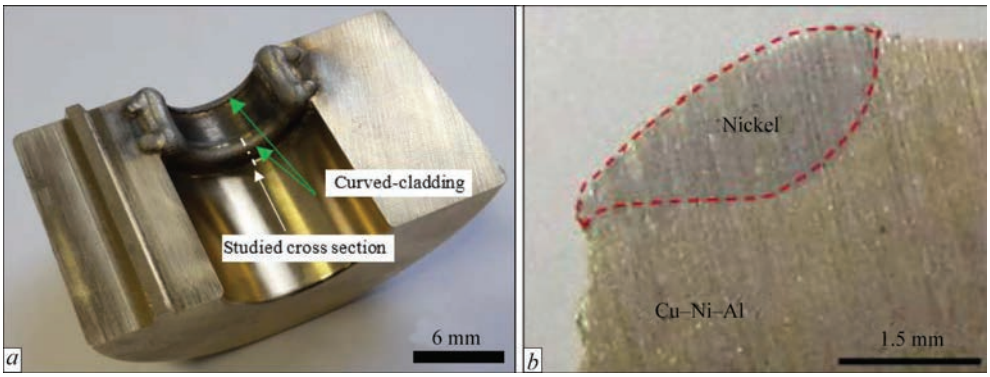

Figure 1. Half of the mold ring after Ni-laser cladding (*a*) and studied cross section (*b*)

ing. Many researches have observed that according to the powder nature, a high power attenuation can appear [11, 12]. There are two ways of describing the dilution (rate) [13]: in geometrical terms, it in calculating the ratio between the melted area (including the HAZ) and the coating area. The second is in metallurgical terms, which consists in measuring the depth of the chemical mixture between the coating and the substrate. Liu et al. [14] present a dilution rate by using the geometrical method during laser cladding of magnesium alloys. According to them, a very low dilution rate prevents from good metallurgical bonding. Using the same definition of the dilution rate, Luo et al. [15] present the same observation during laser cladding of NiCrBSi. Balu et al. [7] used the metallurgical method to measure the dilution rate during laser cladding of Ni-based powder on a Cu substrate. They found that a high dilution can lead to a high HAZ. Pereira et al. [16] observed that during laser cladding of NiCoCrBSi on stainless steel, a very low dilution zone (metallurgical method) at about 2 μm is enough to obtain a perfect bonding without affecting the substrate mechanical properties (no cracking behavior observed). Many authors [17, 18] presented an EDS analysis to measure the dilution between two materials and its components' chemical evolution.

The main challenge in laser cladding on a copper-based substrate is to obtain good bonding despite the low absorptivity of the substrate [19]. Zhang et al. [20] explained that it was impossible to obtain bonding without preheating, so they pre-heated the substrate to 300 °C. It appears that a compromise must be found to respect both the restricted HAZ and the dilution zone needed to guarantee the cohesion between the coating and the substrate. We should bear in mind that this cohesion is crucial to allow further machining of the repaired mold. Moreover, the coating has to be free of cracks and pores to retain a perfect glass surface.

The aim of this study is to obtain a perfect bonding with a limited or non-existent HAZ after cladding of nickel-based material on a Cu–Ni–Al substrate. The novelty in this process is the laser cladding performed without preheating on a curved surface. Also, the high thermal conductivity of the copper-based material is challenging because it can prevent from obtaining the perfect bonding. This can be achieved by identifying the relationship between the dilution zone (existence and thickness) and the bonding quality with regards to the laser process parameters. A microstructural and chemical analysis of the coating/substrate interface will be conducted. Also, microhardness measurements will be presented. The influence of the Gaussian distribution of Ni powder on the laser power attenuation, and thus on the bonding, will be discussed.

MATERIALS AND EXPERIMENTAL TECHNIQUES

Laser cladding consists in melting an injected powder with a very thin surface layer on the substrate by a laser beam to produce a metallurgical bonding. During this study, a 4KW Nd:YAG laser with a wavelength of 1030 nm was used. An optical fiber with a diameter of 600 μm was used for guiding the beam. Ni powder was injected coaxially into the laser beam [21]. A cross-section of the Cu–Ni–Al mold of the bottle ring is shown in Figure 1, *a* after cladding. Figure 1 *b* describes the typical cross-section that has been metallurgically studied.

During the process, the interaction distance, fs, between the laser and the powder is considered (Figure 2).

At the focal plane (position B), the powder flow follows a Gaussian distribution. This has been proved by many research studies [22–24]. In the present study, the Gaussian distribution has been centered at the midpoint of the mold curved surfaces of the samples.

The chemical compositions of the powder and the substrate are listed in Table 1.

The process parameters used during this study are presented in Table 2. These samples are extracted using Taguchi design of experiment. Only samples with a partial or perfect bonding have been selected.

To be characterized, samples were mechanically polished using SiC papers and then diamond polished

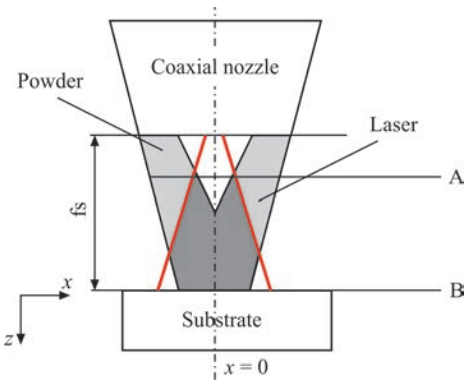

Figure 2. Powder distribution according to the focal position fs [19]

to 1 μm for Optical Microscopy (OM), Scanning Electron Microscopy (SEM) and Energy Dispersive Spectroscopy (EDS) analyses. To operate Electron Backscatter Diffraction (EBSD), an extra OPS polishing was done. Vickers hardness tests were performed on the cross-section, along a line perpendicular to the coating surface with a 10-gf load for 15 seconds. The measurements were taken from either side of the interface for all the 6 samples.

RESULTS AND DISCUSSION

MICROSTRUCTURE FEATURES AND ASSOCIATED CHEMICAL AND MECHANICAL PROPERTIES

Figure 3 describes the three different kinds of bonding behavior that can be observed after laser cladding of Ni-based powder on a Cu–Ni–Al substrate: perfect bonding (Figure 3, *a*), partial bonding (Figure 3, *b*) where the bonding is partially present at the interface and no bonding (Figure 3, *c*). A bonding is considered partial when 15 % bonding default is observed in the coating/substrate interface.

Figure 4 shows the SEM-BSE (Back-Scattered Electrons) analysis of the CNC 5 and CNC 6 samples (see Table 2). Figure 4*a* shows that CNC 5 presents perfect bonding (case of Figure 3, *c*) whereas Figure 4b shows a sample (CNC 6) with a discontinuous bonding (Figure 3, *b*). Indeed, in the curved center, there is a lack of bonding. No analyses have been performed on samples with no bonding (Figure 3, *a*) since the clad is easily separated from the substrate.

For both samples, the substrate is composed of a dendritic matrix. No heat affected zone (HAZ) seems to be present in the substrate because no microstructure modification is noticeable close to the interface. Concerning the Ni deposit, elongated grains are observed along solidification direction for both cases. Small grains can be seen in the coating close to the interface and at the extreme surface.

Figure 5 shows an EBSD analysis of the microstructure and texture around the interface (black squares in Figure 4, *a*, *b*) for both samples (perfect or partial bonding) in order to observe the differences according to the bonding quality.

It can be observed that microstructure is very similar in both cases (Figure 5, *a*, *b*).The solidification features are in accordance with the literature [25–28].

Table 1. Chemical compositions of the substrate and powder

Elements (wt.%)	Fe	Mn	Al	Ni	Zn	Pb	Sn	Si	Cu	B	Cr	C
Cu–Ni–Al	<1	0.5	8.5	15	8	<0.1	0.15	1	Bal	–	–	–
Ni powder	1	0.1	–	Bal	–	–	–	2.5	–	1.7	0.3	0.5

Table 2. Process parameters

Sample	Power, W	Speed, mm/s	Powder feeding rate, g/min	Spot diameter, mm
CNC 1	2400	6.5	26.5	4
CNC 2	2600	10	24.5	3
CNC 3	2800	6.5	32.5	3
CNC 4	2800	8.5	24.5	4
CNC 5	3200	8.5	28.5	3
CNC 6	3200	10	30.5	4

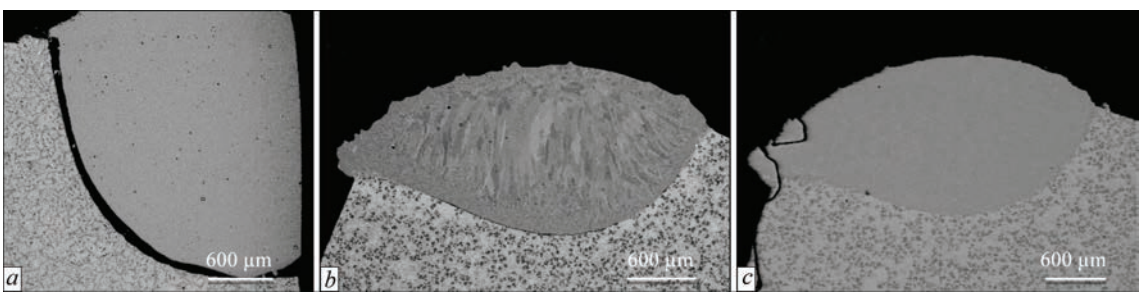

Figure 3. Three kinds of bonding behavior: *a* — no bonding; *b* — partial bonding; *c* — perfect bonding

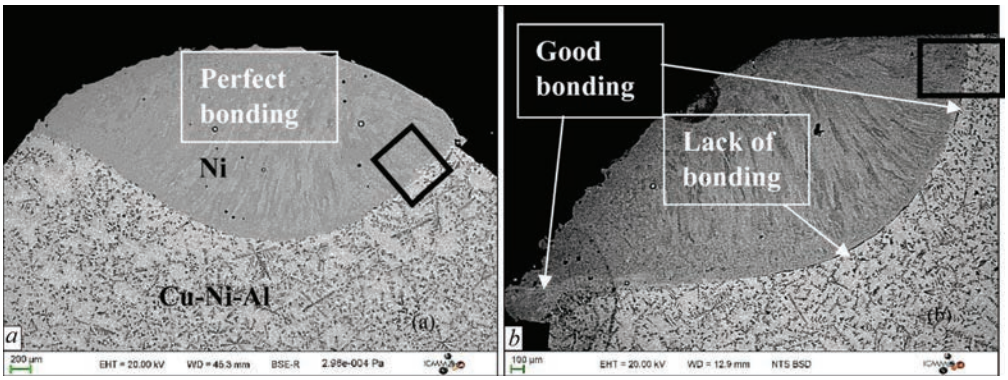

Figure 4. Typical microstructure of the cross-section of the samples: *a* — CNC 5 with good bonding; *b* — CNC 6 with partial bonding obtained by SEM-BSE

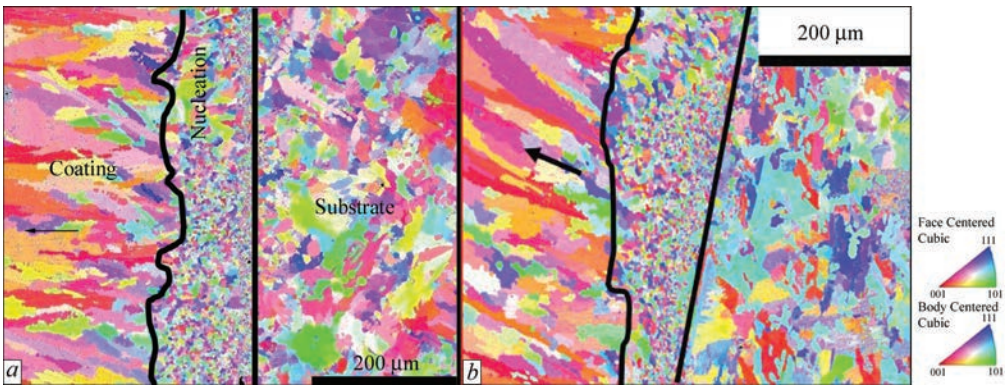

Figure 5. Crystallographic axes parallel to the solidification direction (black arrows): *a* — EBSD analysis of the black square area in Figure 4, *a*, *b*

A nucleation phase, characterized by small equiaxed grains, is evidenced at the interface, then a columnar growth directed mainly parallel to the <001> direction of the dendrites is observed (Figure 5, *a*). So, the bonding quality does not change the solidification behavior during laser cladding.

A SEM-EDS analysis is presented (Figure 6) to observe the chemical impact of the laser cladding at the interface nucleation/substrate.

In the Figure 6, *a*, *b*, deconstruct dendrites from the substrate are observed in a mixed zone at the coating/substrate interface delimited by white lines. Also, the Figure 6, *c* clearly shows a local chemical mixture where copper seems to be replaced by nickel over a thin layer of the substrate. This can be the consequence of a local fusion of the substrate and correspond to the dilution zone that has been reported in the literature [17, 26]. Apart from this area, there are no discernible chemical changes in the substrate or the Ni coating. So, no HAZ can be chemically observed in this study.

A measurement of the dilution zone thickness was made by chemical analysis from the coating to the substrate (Figure 7).

A diminution of the Ni element from the coating to the substrate can be observed. At the same time, the Cu composition progressively increases. Overall, Ni is at around 96 % in the coating, then decreases down to 40 % close to the interface and stays below 10 % in the substrate matrix except inside the dendrites where the Ni increases to 39 %. The dendrites also present a higher level of Al (the high concentration of Ni and Al inside the dendrites is in accordance with Figure 6).

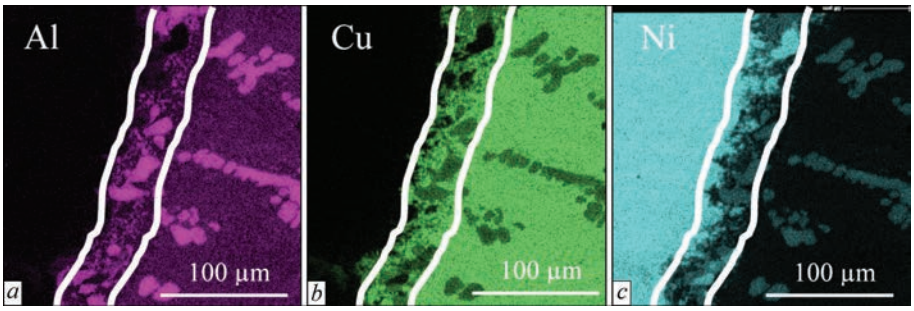

Figure 6. EDS maps of the principal chemical elements composing the deposit and the substrate of sample CNC6: *a* — Al; *b* — Cu; *c* — Ni

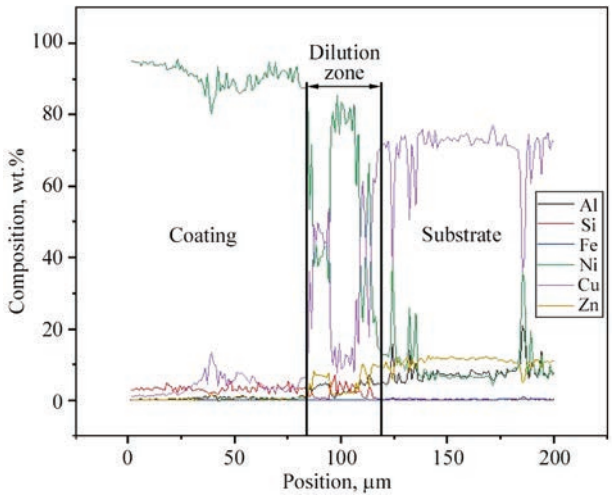

Figure 7. Chemical composition of the dilution zone from the coating to the substrate (sample CNC 6)

The dilution zone exhibits a chemical mixture over about 35 µm for this sample.

Figure 8 shows the hardness measurements through the interface for four typical features of the microstructure: the columnar zone of the coating, the nucleation zone, the dilution zone, and the substrate.

It can be observed from Figure 8 that the micro-hardness of the dilution zone increased to 618 *HV*. The similar results was observed by Pan et al. [27] when cladding Fe-based powder on a stainless steel substrate in their dilution zone. This high hardness in the dilution zone could be explained by the formation of an eutectic of Ni–Ni_3B due to the low ratio of Si/B (≈1.3) in this area as described by Hemmatie et al. [28]. Indeed, they mention that this compound is of high hardness. In the coating and the substrate, the values are not higher than 317 *HV*. This hardness does not indicate the presence of the HAZ in the substrate. No increase of the hardness is noticed in the nucleation area despite the presence of small grains. In fact, the Hall and Petch law which describes that the hardness is higher when the grain size is lower [29]. But this couldn't be verified is the present work.

Since the dilution zone can be quantified using the EDS analysis it could be interesting to observe its evolution along the curved interface in order to corroborate its existence/thickness with the metallurgical bonding quality.

DILUTION ZONE THICKNESS ALONG THE CURVED INTERFACE

To state if the discontinuous bonding along the interface in the studied section is linked to the chemical dilution presence or thickness, a protocol of systematic DZ quantification has been implemented across the section of all samples and is presented in Figure 9. Five lines separated from each other by an angle of 22.5° along which the chemical composition have been measured from the coating to the substrate within 400 µm, and where the DZ depth has been determined. This method allows to plot the DZ evolution along the curved interface (Figure 9).

Figure 9 reveals that the DZ evolution is the same across the section for all the samples studied. On the zones a and e (the edges), the DZ depth is maximum (from 25 to 175 µm according to the cladding parameters). It decreases at lower levels (b and d zones) to between 3 and 21 µm. Then at the center of the curve (c zone) this DZ is minimum (zero in the case of no bonding). Moreover, for all the studied samples, the bonding is lower at the center of the curved section. Therefore, it is possible to draw a direct connection between DZ depth and bonding quality. Indeed, the deeper the DZ, the better the bonding will be. The discontinuous bonding is well highlighted by the DZ evolution along the curve of the cross-section. It is important to understand what phenomenon leads systematically to a weaker chemical dilution at the section curve center during laser cladding, as a function of process parameters.

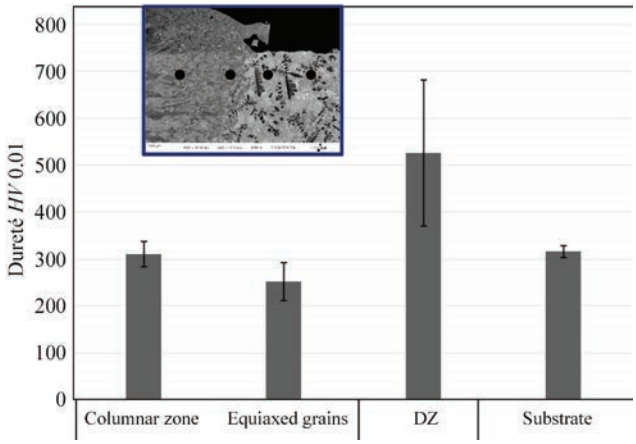

Figure 8. Hardness measurements corresponding to the characteristic features encountered from the coating to the substrate (black points)

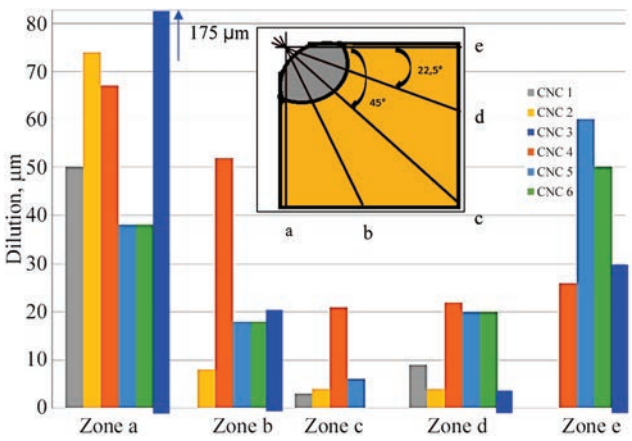

Figure 9. Measurement of the DZ depth over the entire cross-section and DZ depth along the five black lines for all the samples

POWER ATTENUATION

It is well known in the laser cladding process that powder particles contribute to attenuate the incident laser power. Obviously for full consideration it is necessary to calculate the total heat balance of laser surfacing using filler powder, the total amount of heat released by the laser is spent on heating and melting the filler powder, heating the base metal before melting and maintaining the weld pool in a liquid state (the useful part of the heat), as well as radiation into the surrounding space (including as a result of reflection from powder particles, depending on its reflectivity) and heat removal to the base metal (heat loss). The thermal efficiency of the laser surfacing process and the parameters of its regime depend on these indicators: laser power, the amount of powder supplied per unit time, its granulometric composition, etc. [30, 31]. This is complex calculation and for simplification of the description in current research we have considered only the effect of the powder particles (i.e. filler powder). Tabernero et al. [32] have described the impact of a shadow of particles during the interaction of the laser and the powder while cladding is in progress. They have assessed the attenuation undergone by the beam and characterized the density of energy that reaches the surface of the substrate. They were able to perform this calculation with a computational fluid dynamics (CFD) model, which has been experimentally validated. Moreover, the present authors used the calculation of the attenuated power to determine the minimum power necessary to ensure an accurate clad/substrate bonding [26]. Nevertheless, the local attenuation due to the Gaussian powder distribution has not been studied along the curve section.

El Cheikh et al. [23] have discovered that at the focal position, fs, presented in Figure 2, a Gaussian distribution of powder can be observed. Qi et al. [33] have proposed an equation of the powder distribution $N(x, y)$ depending on the radial distance x and the axial distance z in the case of a coaxial nozzle as shown:

$$N(x,z) = N_{\max}(z)\exp\left(-2x^2 / R^2\right), \quad (1)$$

where N_{max}, m^{-3} the peak concentration at the center of powder flow ($x = 0$); x, mm the radial distance; R, mm the powder stream.

To understand how the power is impacted, the Beer Lambert Law can be applied [33, 34]:

$$P'_z(x,z) = P_z(x)\exp(-\alpha SNz), \quad (2)$$

where P'_z W the power attenuated by the powder flow, P'_z W the initial input power during laser cladding; S mm^2 the particle section and α a factor which considers phenomena like the scattering effect, plasma generation. α was obtained from an experiment of the attenuated power during laser cladding. A power meter is placed under an optically neutral glass to protect it from the powder injected. During the test, an air flow was injected horizontally in order to deflect the projected powder. As an example, for an incident measured power of 1916 W, the measured attenuated power was 1498 W for a PFR of 28.5 g/min. This led to adjusting the α coefficient at a value of 6 (this result is in accordance with literature [32]). If α is equal to 1, the attenuation is only due to particle shadow. The present value of 6 indicates that other phenomena (scattering effect, plasma generation) also contribute to the power attenuation.

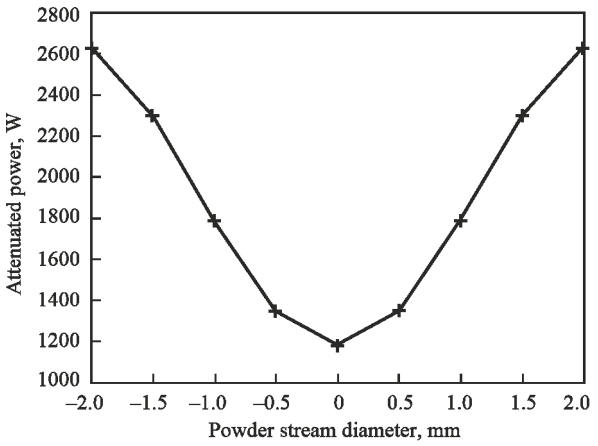

Figure 10. Distribution of the power attenuation on the substrate ($x = 0$ is the focal point) for an input laser power of 2800 W

By inputting the powder distribution on each position of x it is possible to observe the power attenuation on the radial distance for an incident power of 2800 W as an example (Figure 10).

Figure 10 indicates that, at the center of the powder flow (the focal point fs, Figure 2), the power is attenuated from 2800 to 1200 W. At the center of the powder flow ($x = 0$), 57 % of the power is lost due to the powder flow (absorbed or reflected). So, only 43 % is available for the fusion. Moreover, given that the absorptivity of Cu-based materials is about 0.06, only 72 W remains to reach the substrate (and probably melt it). Since the focal plane of the powder flow corresponds to the center of the mold curved surface, it can be assumed that this shadow effect explains the lack of dilution DZ observed at this position. Therefore, this phenomenon may be at the origin of the absence of bonding for some cladding conditions with too weak incident laser power.

A LINK BETWEEN POWER ATTENUATION, DILUTION AND HAZ

No HAZ was observed here when laser cladding on a Cu-based substrate. But the heterogeneous dilution in the mold's curved section can lead to a lack of bond-

ing at the curved center and induce the coating fall out during machining [1]. In the meantime, on the edges (according to the input laser power), less powder generates more power available for the interface fusion. According to the substrate composition, a high HAZ can be generated and induces a cracking behavior due to the high hardness as it was observed in previous researches conducted by the authors during laser cladding on cast iron [35].

CONCLUSION

Ni-based powder was deposited by laser cladding on a Cu-based substrate with a curved surface. The cladding process parameters were widely explored in order to verify the bonding quality of the clad to the substrate. Three kinds of metallurgical bonding have been noted: lack of bonding, partial bonding or perfect bonding. In addition, a constant lack of bonding is observed in the center of the substrate curved surface. Moreover, the chemical dilution depth between Ni and Cu was measured at the interface clad/substrate depending on process parameters. It appears that the dilution depth is also lower at the same location of the curved surface. This could be explained by the Gaussian distribution of the powder flow around this point. Indeed, at the curved center the powder density is at maximum, so the input laser power is significantly attenuated. Less energy is then available for the substrate to melt and to ensure a perfect metallurgical bonding. The attenuated power evolution moving away from this central point would explain the discontinuous bonding along the interface in the cross-section. As it was mentioned above, a compromise was found in the present work to ensure a minimal dilution (DZ) in the curved center without affecting the based material properties (limit the HAZ). This optimization can correspond for example to a laser power of 3200 W with a PFR of 28.5 g/min and a scanning speed of 8.5 mm/s.

ACKNOWLEDGMENTS

The authors wish to thank C. Aboud, N. Barbosa and C. Lafarge from the ETS CHPOLANSKY for their help in the sample elaboration by laser cladding and their great skill in the field of this technology applied to non-planar surfaces. This research was supported by the ANRT (French National Agency for Research and Technology) and ETS Chpolansky.

REFERENCES

1. Rege, M., Van Linden, S. (2016) *Stage de formation aux techniques de rechargement dans l'industrie verrière*, Marcoussis.
2. Oberländer, B.C., Lugscheider, E. (1992) Comparison of properties of coatings produced by laser cladding and conventional methods. *Mater. Sci. Technol. (United Kingdom)*, **8**, 657–665. DOI: https://doi.org/10.1179/mst.1992.8.8.657.
3. Steen, W.M., Mazumder, J. (2010) *Laser Material Processing*. 4th Ed., Springer.
4. Ryabtsev, I.A., Perepletchikov, E.F. (1992) *Properties of alloys based on Fe, Ni, Co, deposited by laser-powder method. Sat. on Deposited metal. Composition, structure and properties*. Kyiv, E.O. Paton Electric Welding Institute of the NASU, 23–26.
5. Arabi Jeshvaghani, R., Jaberzadeh, M., Zohdi, H., Shamanian, M. (2014) Microstructural study and wear behavior of ductile iron surface alloyed by Inconel 617. *Mater. Des*., **54**, 491–497. DOI: https://doi.org/10.1016/j.matdes.2013.08.059.
6. Liu, H., Hao, J., Han, Z. et al. (2016) Microstructural evolution and bonding characteristic in multi-layer laser cladding of NiCoCr alloy on compacted graphite cast iron. *J. Mater. Process. Technol*., **232**, 153–164. DOI: https://doi.org/10.1016/j.jmatprotec.2016.02.001.
7. Balu, P., Rea, E., Deng, J. (2015) Laser cladding of nickel-based alloy coatings on copper substrates. In: *Proc. of SPIE,* **9657**, 1–10. DOI: https://doi.org/10.1117/12.2175966
8. Saqib, S., Urbanic, R.J., Aggarwal, K. (2014) Analysis of laser cladding bead morphology for developing additive manufacturing travel paths. *Procedia CIRP*, **17**, 824–829. DOI: https://doi.org/10.1016/j.procir.2014.01.098.
9. Tao Y.F., Li J., Lv Y.H., Hu L.F. (2017) Effect of heat treatment on residual stress and wear behaviors of the TiNi/Ti-2Ni based laser cladding composite coatings. *Opt. Laser Technol.*, **97**, 379–389. DOI: https://doi.org/10.1016/j.optlastec.2017.07.029.
10. Kim, C.K., Choi, S.G., Kim, J.H. et al. (2020) Characterization of surface modification by laser cladding using low melting point metal. *J. Ind. Eng. Chem.*, **87**, 54–59. DOI: https://doi.org/10.1016/j.jiec.2020.03.010.
11. Kumar, S., Roy, S. (2006) The effect of Marangoni-Rayleigh-Benard convection on the process parameters in blown-powder laser cladding process-A numerical investigation, Numer. *Heat Transf. Pt A Appl.*, **50**, 689–704. DOI: https://doi.org/10.1080/10407780600605286.
12. Rienstra, S.W., Chandra, T. (2001) Analytical approximations to the viscous glass-flow problem in the mould-plunger pressing process, including an investigation of boundary conditions. *J. Eng., Math*. **39**, 241–259. DOI: https://doi.org/10.1023/A:1004883310709 CITATIONS.
13. Toyserkani, E., Amir, K., Stephen, C. (2006) *Laser Cladding, CRC PRESS.*
14. Liu, J., Yu H., Chen, C. et al. (2017) Research and development status of laser cladding on magnesium alloys: A review. *Opt. Lasers Eng.*, **93**, 195–210. DOI: https://doi.org/10.1016/j.matdes.2014.01.077.
15. Luo, X., Li, J., Li, G.J. (2015) Effect of NiCrBSi content on microstructural evolution, cracking susceptibility and wear behaviors of laser cladding WC/Ni–NiCrBSi composite coatings. *J. Alloys Compd*., **626**, 102–111. DOI: https://doi.org/10.1016/j.jallcom.2014.11.161.
16. Pereira, J.C., Zambrano, J.C., Rayón, E. et al. (2018) Mechanical and microstructural characterization of MCrAlY coatings produced by laser cladding: The influence of the Ni, Co and Al content. *Surf. Coatings Technol.*, **338**, 22–31. DOI: https://doi.org/10.1016/j.surfcoat.2018.01.073.
17. Adesina O.S., Obadele B.A., Farotade G.A. et al. (2020) Influence of phase composition and microstructure on corrosion behavior of laser based Ti–Co–Ni ternary coatings on Ti–6Al–4V alloy. *J. Alloys Compd.*, **827**, 1–11. DOI: https://doi.org/10.1016/j.jallcom.2020.154245.
18. Wang, S., Liu, C. (2019) Real-time monitoring of chemical composition in nickel-based laser cladding layer by emission spectroscopy analysis. *Materials (Basel)*, **12**, 1–15. DOI: https://doi.org/10.3390/ma12162637.

19. Babinets, A.A., Ryabtsev, I.O., Lentyugov, I.P. et al. (2020) Problems and prospects of surfacing of copper and copper parts by wear-resistant layers (Review). *The Paton Welding J.*, **5**, 15–23. DOI: https://doi.org/10.37434/tpwj2020.05.03
20. Zhang, Y., Tu, Y., Xi, M., Shi, L. (2008) Characterization on laser clad nickel based alloy coating on pure copper. *Surf. Coatings Technol.*, **202**, 5924–5928. DOI: https://doi.org/10.1016/j.surfcoat.2008.06.163
21. F. Bourahima, A. Helbert, M. Rege, V. Ji, D. Solas, et al. (2019) Laser cladding of Ni based powder on a Cu–Ni–Al glassmold: Influence of the process parameters on bonding quality and coating geometry. *J. of Alloys and Compounds*, Elsevier, **771**, 1018–1028. DOI: https://doi.org//10.1016/j.jallcom.2018.09.004
22. Ferreira, E., Dal, M., Colin, C. et al. (2020) Experimental and numerical analysis of gas/powder flow for different LMD nozzles. *Metals (Basel)*, **10**, 1–20. DOI: https://doi.org/10.3390/met10050667.
23. Cheikh, H. El, Courant, B., Branchu, S. et al. (2012) Analysis and prediction of single laser tracks geometrical characteristics in coaxial laser cladding process. *Opt. Lasers Eng.*, **50**, 413–422. DOI: https://doi.org/10.1016/j.optlaseng.2011.10.014.
24. Pouzet, S., Peyre, P., Gorny, C. et al. (2016) Additive layer manufacturing of titanium matrix composites using the direct metal deposition laser process. *Mater. Sci. Eng. A*, **677**, 171–181. DOI: https://doi.org/10.1016/j.msea.2016.09.002.
25. Song, B., Yu, T., Jiang, X. et al. (2020) The relationship between convection mechanism and solidification structure of the iron-based molten pool in metal laser direct deposition. *Int. J. Mech. Sci.*, **165**, 1–14. DOI: https://doi.org/10.1016/j.ijmecsci.2019.105207.
26. Pereira, J.C., Zambrano, J.C., Tobar, M.J. et al. (2015) High temperature oxidation behavior of laser cladding MCrAlY coatings on austenitic stainless steel. *Surf. Coatings Technol.*, **270**, 243–248. DOI: https://doi.org/10.1016/j.surfcoat.2015.02.050.
27. Pan, C., Li, X., Zhang, R. et al. (2021) Research on microstructural and property evolution in laser cladded HAZ. *Surf. Eng.*, **37**, 1514–1522. DOI: https://doi.org/10.1080/02670844.2021.1929737.
28. Hemmati, I., Ocelík, V., De Hosson, J.T.M. (2013) Effects of the alloy composition on phase constitution and properties of laser deposited Ni–Cr–B–Si coatings. *Phys. Procedia.*, **41**, 302–311. DOI: https://doi.org/10.1016/j.phpro.2013.03.082.
29. Gourges-Lorenzon, A.-F. (1972) Durcissement et renforcement des materiaux. *Matériaux Pour l'ingénieur*, 159–170.
30. Gladkiy, P.V., Perepletchikov, E.F., Ryabtsev, I.A. (2007) *Plasma welding*. Kyiv.
31. Kuskov, Yu.M., Ryabtsev, I.A., Kuzmenko, O.G., Lentyugov, I.P. (2020) *Electroslag technologies for surfacing and recycling of metal and metal-containing wastes*. Kyiv.
32. Tabernero, I., Lamikiz, A., Martínez, S. et al. (2012) Modelling of energy attenuation due to powder flow-laser beam interaction during laser cladding process. *J. Mater. Process. Technol.*, **212**, 516–522. DOI: https://doi.org/10.1016/j.jmatprotec.2011.10.019.
33. Qi, H., Mazumder, J., Ki, H. (2006) Numerical simulation of heat transfer and fluid flow in coaxial laser cladding process for direct metal deposition. *J. Appl. Phys.*, **100**, 1–11. DOI: https://doi.org/10.1063/1.2209807.
34. Peyre, P., Aubry, P., Fabbro, R. et al. (2008) Analytical and numerical modelling of the direct metal deposition laser process. *J. Phys. D. Appl. Phys.*, **41**, 1–10. DOI: https://doi.org/10.1088/0022-3727/41/2/025403.
35. Bourahima, F., Helbert, A., Ott, F. et al. (2021) *Multi-scale characterization by neutronography and electron diffraction of Ni coating on Cu–Ni–Al or cast-iron glass molds after laser cladding*. Trans Tech Publ. Ltd., **1016**, 297–302.

ORCID

F. Bourahima: 0000-0003-2459-7799,
T. Baudin: 0000-0002-6765-360X,
V. Ji: 0000-0003-1979-7323
F. Brisset: 0000-0003-0952-2748,
A. Zavdoveev: 0000-0003-2811-0765
A.L. Helbert: 0000-0003-1679-9569

CONFLICT OF INTEREST

The Authors declare no conflict of interest

CONFLICT OF INTEREST

The Authors declare no conflict of interest

CORRESPONDING AUTHOR

A. Zavdoveev
E.O. Paton Electric Welding Institute of the NASU
11 Kazymyr Malevych Str., 03150, Kyiv, Ukraine.
E-mail: paton39@ukr.net

SUGGESTED CITATION

F. Bourahima, T. Baudin, M. Rege, V. Ji, F. Brisset, A. Zavdoveev, A.L. Helbert (2022) Formation of a joint between deposited and base metals during laser cladding of a nickel-based powder onto a copper-based alloy. *The Paton Welding J.*, **4**, 26–33.

JOURNAL HOME PAGE

https://pwj.com.ua/en

Received: 22.03.2022
Accepted: 30.06.2022

APRIL 24, 2014 A sculptor under the pseudonym of TEJN installed one of his latest sculptures — «Reaching for Freedom». TJEN is the pseudonym of a contemporary Danish artist, who began his artistic work as a street artist in 2007. Making his works from metal and using welding, he became famous owing to unsanctioned creation of sculptures. Without permission of the authorities, the artist welds or chains the monument, wherever he wants. Later on the sculptures began to be returned to their places as architectural monuments. In his work the sculptor uses welding, cutting, surfacing and other methods of metal treatment. Today his works are often displayed at prestigious exhibitions.